Rate enhancement of bacterial extracellular electron transport involves bound flavin semiquinones

Akihiro Okamoto[a], Kazuhito Hashimoto[a,b,1], Kenneth H. Nealson[c,d], and Ryuhei Nakamura[a,1]

[a]Department of Applied Chemistry, School of Engineering, The University of Tokyo, Tokyo 113-8656, Japan; [b]Hashimoto Light Energy Conversion Project, Exploratory Research for Advanced Technology, Japan Science and Technology Agency, Tokyo 113-8656, Japan; [c]Departments of Earth Sciences and Biological Sciences, University of Southern California, Los Angeles, CA 90089; and [d]Craig Venter Institute, San Diego, CA 92121

Edited* by J. Woodland Hastings, Harvard University, Cambridge, MA, and approved March 5, 2013 (received for review November 29, 2012)

Extracellular redox-active compounds, flavins and other quinones, have been hypothesized to play a major role in the delivery of electrons from cellular metabolic systems to extracellular insoluble substrates by a diffusion-based shuttling two-electron-transfer mechanism. Here we show that flavin molecules secreted by *Shewanella oneidensis* MR-1 enhance the ability of its outer-membrane *c*-type cytochromes (OM *c*-Cyts) to transport electrons as redox cofactors, but not free-form flavins. Whole-cell differential pulse voltammetry revealed that the redox potential of flavin was reversibly shifted more than 100 mV in a positive direction, in good agreement with increasing microbial current generation. Importantly, this flavin/OM *c*-Cyts interaction was found to facilitate a one-electron redox reaction via a semiquinone, resulting in a 10^3- to 10^5-fold faster reaction rate than that of free flavin. These results are not consistent with previously proposed redox-shuttling mechanisms but suggest that the flavin/OM *c*-Cyts interaction regulates the extent of extracellular electron transport coupled with intracellular metabolic activity.

iron-reducing bacteria | electromicrobiology | microbial fuel cell | whole-cell voltammetry | flavin mononucleotide

Bacterial extracellular electron transport (EET) to solid electron acceptors, such as Fe(III)- and Mn(IV)-oxide minerals and artificial electrodes, represents a central driving force for geochemical mineral cycling and bioelectrical systems (1–3). The metal-reducing bacterium *Shewanella oneidensis* MR-1 is one of the most extensively studied organisms for understanding such EET processes (4–6). MR-1 expresses a significant quantity of cell-surface redox-active proteins, namely the *c*-type cytochromes (*c*-Cyts), which form a hypothetical protein complex "OmcA–MtrCAB" (6, 7) in which these proteins work together to transport electrons generated by the intracellular metabolic oxidation of organic matter to solid extracellular electron acceptors as a terminal process in microbial respiration (8–10). The electron transfer (ET) chain from the inner to outer membrane (OM) is called the metal reduction (Mtr) pathway and is responsible for both metal-oxide reduction reactions and anodic current production in microbial fuel cells (MFCs) (5, 9). In addition, it has been proposed that secreted flavins, for example riboflavin (RF) and/or flavin mononucleotide (FMN), are reduced by MR-1 cells and then in their free form function as redox mediators for the Mtr pathway, thus facilitating EET reactions (Fig. 1*A*) (11, 12). In support of this hypothesis, it was reported that the removal of flavin from the supernatants of systems with electrode-bound biofilms resulted in an ~80% loss in microbial current production (12). Moreover, the addition of micromolar amounts of riboflavin to a *Shewanella*-based MFC led to a nearly 10-fold increase in current production (10).

Studies using purified proteins have revealed that flavins specifically accelerate the enzymatic reduction of iron oxides and electrodes through interaction with the OM protein MtrC, which is a 71-kDa decaheme *c*-Cyt and a main component of the Mtr pathway in *Shewanella* (13–15). Consistent with this observation, mutant strains lacking MtrC are significantly impaired in flavin-mediated reduction ability (10). Furthermore, the removal of flavins bound to MtrC decreased its enzymatic activity by three orders of magnitude (15). Accordingly, detailed crystal analysis of MtrC homology protein suggested that the flavin can access heme centers either exposed to the exterior or buried in the protein scaffolds of MtrC (14). Although these results demonstrated that flavins serve as primary electron acceptors for the reduced hemes of the MtrC protein, the mechanism by which flavins facilitate the Mtr pathway has remained enigmatic and is still the subject of debate.

S. oneidensis MR-1 cells reportedly use flavins as a two-electron/proton redox mediator, that is, $FMN + 2e^- + 2H^+ \rightarrow FMNH_2$ (12) (Fig. 1*A*). However, the redox potential of FMN/$FMNH_2$ is −220 mV [vs. the standard hydrogen electrode (SHE)], which is 270 mV more negative than that for in vivo OmcA–MtrCAB protein complexes (16), resulting in a strong endergonic ET reaction. Although the broad-potential redox window of MtrC protein possibly allows the enzymatic reduction of flavins (14), this energy balance apparently conflicts with the reported observations that flavins accelerate EET via the Mtr pathway. Thus, it is reasonable to assume that MR-1 cells use flavins in a different manner from the proposed free-flavin-mediated electron-shuttling mechanism to overcome this energetic barrier. Here we report studies focused on the elucidation of the mechanism(s) by which flavin molecules accelerate the EET process through the interaction with MtrC protein.

As in previous studies (16, 17), we have used whole-microorganism voltammetry to examine the redox characteristics of biological ET components under in vivo conditions. Differential pulse voltammetry (DPV) is capable of detecting nanomolar levels of substrates by minimizing nonfaradaic current (18) and is therefore one of the most suitable voltammetric techniques for monitoring redox species present in trace amounts in biological systems (12). To accomplish this, we fabricated a monolayer biofilm of MR-1 cells on highly uniform and flat indium tin-oxide (ITO) electrodes and conducted DPV measurements to elucidate the redox properties of flavin associated with MtrC protein scaffolds. Our analyses revealed that the energetics and kinetics of the EET via the MtrC-bound FMN is markedly different from those reported for the electron-shuttling process (Fig. 1*B*). For the mechanism and origin of the redox property alteration in flavin, we also examined how FMNs interact with MtrC protein scaffolds. Not surprisingly, we have seen similar, but not identical, results for the interaction of RF.

Author contributions: A.O. and R.N. designed research; A.O. performed research; A.O. contributed new reagents/analytic tools; A.O. analyzed data; A.O., and K.H., K.H.N., and R.N. wrote the paper.

The authors declare no conflict of interest.

Freely available online through the PNAS open access option.

*This Direct Submission article had a prearranged editor.

See Commentary on page 7537.

[1]To whom correspondence may be addressed. E-mail: hashimoto@light.t.u-tokyo.ac.jp or nakamura@light.t.u-tokyo.ac.jp.

This article contains supporting information online at www.pnas.org/lookup/suppl/doi:10.1073/pnas.1220823110/-/DCSupplemental.

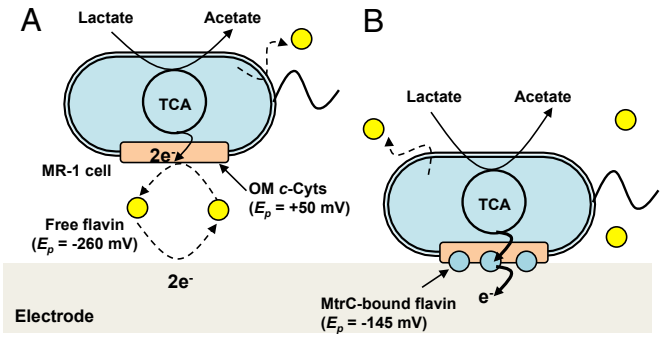

Fig. 1. Schematic illustration of self-secreted flavin molecules to mediate extracellular electron-transport (EET) processes of *S. oneidensis* MR-1. (*A*) Electron shuttling process between OM *c*-Cyt complexes and electrodes by two-electron redox reaction of free-form flavins (peak potential in differential pulse (DP) voltammogram: E_p = −260 mV vs. SHE). Note that the rate of enzymatic reduction of free flavins should be very slow due to the large energy barrier existing between the flavin and OM *c*-Cyt (E_p = +50 mV). (*B*) Direct EET process via a one-electron reaction of flavins (E_p = −145 mV) that are associated with the flavin binding site in OM *c*-Cyt (MtrC protein). A flavin/MtrC interaction facilitates a one-electron redox reaction via semiquinone with a positive shift in the E_p of flavins from −260 mV to −145 mV, resulting in a highly faster EET rate than that observed for a two-electron EET process.

Results

Redox Properties of FMN at the Cell/Electrode Interface. To elucidate the redox properties of flavin molecules associated with MtrC at the cell/electrode interface, whole-cell voltammetry measurements were conducted with monolayer biofilms of *S. oneidensis* MR-1 grown on an ITO electrode. For the experiment, a cell suspension of GFP-labeled bacteria with an optical density at λ = 600 nm (OD_{600}) of 0.1 was cultivated on an ITO electrode poised at +200 mV (vs. Ag/AgCl KCl saturated) in the presence of lactate as an energy source. After 25 h of incubation, confocal fluorescence microscopy showed the formation of a monolayer biofilm with a thickness of less than 1 μm on the electrode surface (Fig. S1*A*), with almost no planktonic cells (17).

We next subjected the MR-1 biofilm to DPV by stepping the electrode potential from −0.4 to +0.4 V (vs. SHE) in 5-mV increments (Fig. 2). As shown in Fig. 2*A*, the differential pulse (DP) voltammograms obtained for the monolayer biofilm contained two anodic peaks at redox potentials (E_p) of +50 mV and −145 mV. Although the former peak has been previously assigned to the OmcA–MtrCAB complex (17), the latter peak is not attributable to the well-characterized redox species of strain MR-1, such as quinones, riboflavin, or FMN (19, 20). When FMN was added to the reactor, the peak current at −145 mV increased in proportion to the concentration of supplemented FMN (Fig. 2*A*), demonstrating that the E_p at −145 mV is assignable to FMN in the monolayer biofilm. Notably, the observed E_p at −145 mV was 115 mV more positive than that observed for the potential of free FMN added to the reactor without bacterial biofilms (−260 mV, Fig. 2*B*). In addition, when we increased the concentration of FMN in the reactor, the E_p gradually shifted to the E_p of free FMN (Fig. S1 *B* and *C*); that is, the redox property of FMN in monolayer biofilms is significantly altered by interaction with the cell.

The number of electrons (n) involved in the redox reaction of FMN with electrodes was estimated from the half-width potential ($\Delta E_{p/2}$) of the DPV signal. For free FMN dissolved in defined medium (DM), the DPV signal exhibited a $\Delta E_{p/2}$ of 60 mV (Fig. 2*B*, trace 1), which is consistent with an n of 2 (21). When fully oxidized flavin (Ox) is reduced in one- and two-electron reactions, the resulting flavin derivatives are called semiquinone (Sq) and hydroquinone (Hq) species, respectively (22–24), as shown in [**1**] and [**2**]:

$$\mathrm{FMN\ (Ox)} + \mathrm{e^-} + \mathrm{H^+} \rightleftarrows \mathrm{FMNH\ (Sq)} \qquad [1]$$

$$\mathrm{FMN\ (Ox)} + 2\ \mathrm{e^-} + 2\ \mathrm{H^+} \rightleftarrows \mathrm{FMNH_2\ (Hq)}. \qquad [2]$$

The $\Delta E_{p/2}$ value obtained here for free FMN indicated that FMN mediated the two-electron redox reaction between Ox and Hq (Ox/Hq) (12). In contrast, the FMN in the monolayer biofilm gave a larger $\Delta E_{p/2}$ relative to free FMN (Fig. 2*B*). The $\Delta E_{p/2}$ of 130 mV is similar to that reported for one-electron transfer reactions (21), indicating that the n of flavin changed from 2 to 1 together with the shift of E_p from −260 mV to −145 mV in the presence of monolayer biofilms. That is, in the presence of biofilms, Sq was generated at the cell/electrode interface. To support the assignment of E_p = −145 mV to Sq, the effect of the addition of the free radical scavenger tocopherol on the DPV signals was examined. Following the addition of 1.0 mM tocopherol to the system containing the monolayer biofilm (25), the peak current at E_p = −145 mV displayed a 30% decrease (Fig. S2), indicating that the peak current was assignable to the oxidation reaction of Sq to Ox.

EPR spectroscopy measurements were conducted to further confirm the assignment of the −145 mV peak. In the presence of 10 mM lactate as an electron donor, a cell suspension of MR-1 containing 16 μM flavin was frozen at 77 K after 1 h of

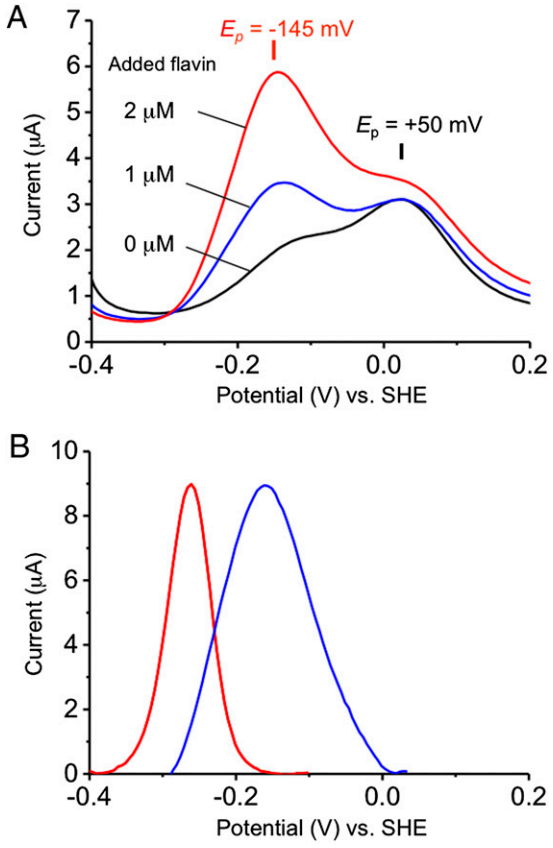

Fig. 2. Redox property of FMN in MR-1 biofilms differs from that of free-form FMN. (*A*) DP voltammograms for monolayer biofilms of *S. oneidensis* MR-1 on an ITO electrode surface in the presence of 0, 1.0, and 2.0 μM FMN. (*B*) Baseline-subtracted DP voltammograms for cell-free DM containing 16 μM FMN (red line). Differences in the peak currents from the voltammograms in *A* with added FMN concentrations of 0 and 1.0 μM (blue line) were normalized with those obtained from the cell-free defined media.

incubation in the presence of Fe_2O_3 particles as an electron accepter. As shown in Fig. 3*A*, paramagnetic species were detected at $g = 2.002$, which is identical to the value reported for semiquinone species in flavoproteins (26), whereas the relatively broad line width reflects the heterogeneous distribution of radical environments (27). In contrast, paramagnetic species were not detectable in the medium lacking lactate (Fig. 3*C*). Because Sq was detected only in the presence of lactate, it seems that the Sq was formed via the reduction of the Ox species by metabolically generated electrons. Furthermore, Sq was not reduced to Hq, even in the absence of Fe_2O_3 particles serving as electron acceptors (Fig. 3*B*). Thus, the E_p at −145 mV was assigned to the one-electron redox couple of Ox and Sq, but not to that of Sq and Hq.

Evidence for the Interaction Between FMN and MtrC. Detailed crystallographic studies of the redox protein Mtr-F (14) have revealed presumptive flavin-binding sites within the MtrC protein scaffold; this is in agreement with the fact that mutant cells incapable of making MtrC exhibit impaired flavin-reduction ability (10). Here, to determine whether Sq specifically associates with the MtrC protein in vivo, monolayer biofilms of mutant strains lacking the ability to produce MtrC (Δ*mtrC*), OmcA (Δ*omcA*), or a biosynthetic protein of capsular polysaccharide (ΔSO3177) were subjected to DPV measurements (Fig. 4 and Fig. S3). As shown in Fig. 4*A*, the DP voltammogram of Δ*mtrC* in the presence of 2.0 μM FMN showed a peak at −240 mV, which was assigned to free FMN (Fig. 4*A*), demonstrating the impaired ability of Δ*mtrC* to produce Sq. In contrast, the positive shift of E_p from −260 to −153 mV and −141 mV was observed for Δ*omcA* and ΔSO3177 (Fig. S3 *A* and *B*), respectively. The lack of OmcA protein provided little effect on the formation of Sq in MR-1. Furthermore, because disruption of the SO3177 gene greatly alters the cell-surface properties of strain MR-1, including the charge and hydrophobicity (28), the formation of Sq did not result from random attachment of FMN on the cellular surface. Together, these results strongly suggest that the Sq (E_p of −145 mV) that is formed during this interaction was stabilized via a specific association with the MtrC protein scaffold.

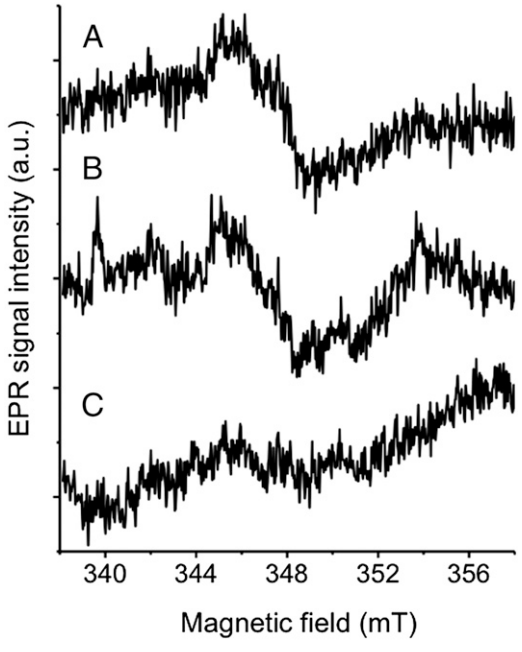

Fig. 3. Effect of an electron donor and accepter in the generation of semiquinone (Sq) free radical in MR-1 cells. Electron spin resonance difference spectrum obtained at 77 K for suspension of *S. oneidensis* MR-1 cells in the presence of 16 μM FMN and 5 mM lactate as an electron donor (*A*) with and (*B*) without added Fe_2O_3 particles as an electron acceptor. For (*C*), lactate was not added into the cell suspension. For all measurements, cell suspensions in 50% glycerol were prepared under anaerobic conditions. The spectrum of the cell suspension with 50% (vol/vol) glycerol was used as reference.

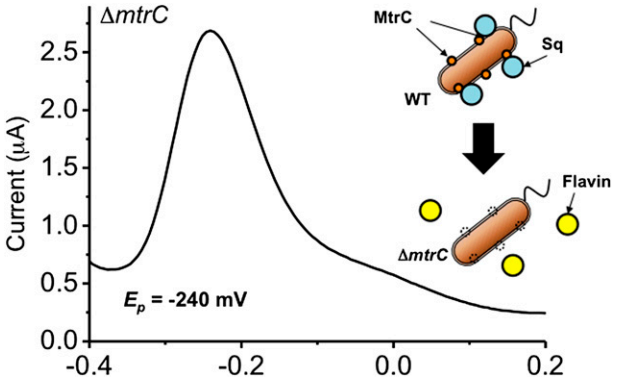

Fig. 4. Role of OM *c*-Cyts (MtrC protein) in Sq stabilization. DP voltammograms of a monolayer biofilm of strains Δ*mtrC* in the presence of 2.0 μM FMN. (*Inset*) Sq represents semiquinone.

Ox/Sq Redox Reaction Involves the Predominant EET Conduit at the Cell/Electrode Interface. Because flavin molecules, when added in excess, markedly accelerate the EET reaction from MR-1 cells to electrodes (10), we also examined the contribution of Ox/Sq couples to the EET process by analyzing the relationship between the amount of Sq and the anodic current (I_{ac}) generated by the metabolic oxidation of lactate. The I_{ac} of monolayer biofilms of strain MR-1 cells was measured at a poised electrode potential of 200 mV (vs. Ag/AgCl), whereas the amount of Sq located at the cell/electrode interface was estimated from the anodic peak current at −145 mV (I_{-145}) in the DP voltammograms (Fig. 5). In the plot of I_{ac} as a function of I_{-145}, I_{ac} exhibited a positive correlation with I_{-145}, as a fitted line passed through the point of origin, giving a square of the correlation coefficient of 0.998 (Fig. 5*A*). This result revealed that the generation of the redox cycling of Ox and Sq accelerates the delivery of respiratory electrons to the ITO electrodes. As a comparison, the contribution of OM *c*-Cyts to the microbial current generation was examined by conducting the same analysis in the absence of added flavin molecules (Fig. 5*B*). In this analysis, I_{ac}, which was plotted as a function of the peak current at +50 mV assigned to OM *c*-Cyts, was not positively correlated with the amount of OM *c*-Cyts. This suggests that the acceleration of EET by flavins at the cell/electrode interface is the consequence of the redox reaction of the Ox/Sq couple bound to the MtrC protein, but not due to an electron-shuttling process of free FMN or direct ET from OM *c*-Cyts to electrodes.

Sq Formation Is Coupled with Metabolic Activity. Under physiological conditions, respiratory electrons are continuously generated by strain MR-1 through the metabolic oxidation of lactate and are transferred to electrodes or extracellular electron acceptors via the Mtr pathway. Thus, I_{ac} reflects the metabolic activity of bacterial cells and is consistent with the notion that most of the hemes in OM *c*-Cyts are present in the reduced form when cells are in the metabolically active state. Here, with an assumption that Sq formation was relevant to the redox states of hemes in MtrC proteins, we analyzed the DPV signals of monolayer biofilms in the presence of increasing concentrations of lactate (Fig. 6). DPV measurements were conducted at different stages of current production, as indicated with arrows in Fig. 6*A*. When cells were grown in the absence of lactate, microbial current maintained

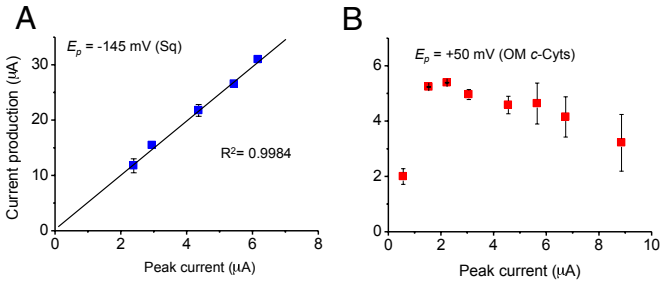

Fig. 5. Contribution of the EET pathway associated with Sq formation in microbial current generation. Plot of bacterial current production at an electrode potential of +200 mV (vs. Ag/AgCl KCl saturated) against the peak current of (*A*) Sq (E_p = −145 mV) and that of (*B*) OM *c*-Cyt (E_p = +50 mV), as determined by DP voltammetry. The squares of the correlation coefficients were estimated by the addition of the point of origin to the obtained data. Error bars indicate the SEMs calculated with microbial current production data obtained before and after a DP voltammetry measurement.

a steady, low value; however, the current sharply increased to 8 μA upon adding 10 mM lactate into the reactor. When the system was producing a low respiratory current (~2 μA), the DP voltammogram of monolayer biofilms gave an E_p at −250 mV (Fig. 6*B*) that was almost identical to the E_p of the two-electron reaction of free FMN. However, when the current displayed a large increase following the addition of lactate, the E_p displayed a prompt shift from −250 to −151 mV (Fig. 6*C*), indicating that the *n* of FMN changed from 2 to 1 through the activation of microbial metabolism. We also confirmed that the E_p of flavin shifted in the opposite direction when metabolic activity decreased. Namely, as shown in DP voltammograms obtained during the stage with a high respiratory current (Fig. S4 *A*, *B*, *D*, and *E*), Sq formation was observed; however, the E_p shifted in a negative direction with a corresponding decrease in I_{ac} due to the cellular consumption of added lactate and the addition of metabolic inhibitor (2-heptyl 4 hydroxyquinoline *N*-oxide) for Mtr pathway (29) (Fig. S4 *C* and *F*). Taken together, these results indicate that Sq formation in the MtrC protein scaffold requires metabolically active bacterial cells.

RF Interacts with OmcA to Mediate EET. Because RF also accelerates the EET reaction from MR-1 cells (10), we examined whether RF facilitates the one-electron EET process via associating with MtrC or OmcA protein. DPV measurements were

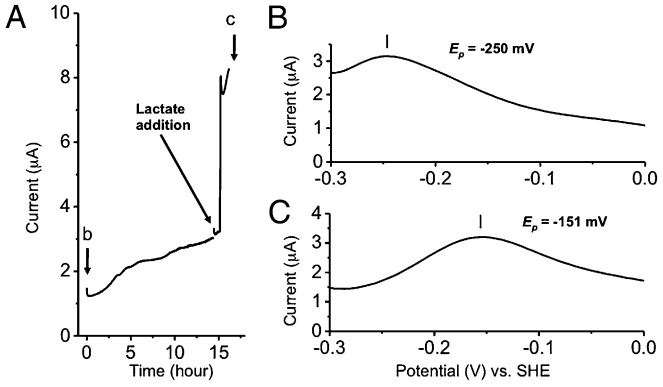

Fig. 6. FMN/MtrC protein interaction couples with metabolic activity. (*A*) Current (I) vs. time measurements of microbial current generation for strain MR-1 cells on an ITO electrode surface at +200 mV (vs. Ag/AgCl KCl saturated). The arrow indicates the point at which 10 mM lactate was added into the reactor. DP voltammograms for monolayer biofilms of *S. oneidensis* MR-1 on an ITO electrode surface with the addition of 2.0 μM FMN, (*B*) before and (*C*) after the addition of lactate.

conducted with monolayer biofilms of WT MR-1, Δ*mtrC*, and Δ*omcA* strain in the presence of 2.0 μM RF. The DP voltammogram of WT provided an E_p at −139 mV (Fig. S5*A*), which was positively shifted from E_p of free RF (E_p = −260 mV) and almost identical to the E_p of a one-electron redox reaction of MtrC-associated FMN. On one hand, as shown in Fig. S5*B*, E_p was observed at −95 mV for Δ*mtrC* deletion mutant. On the other hand, the E_p of RF for Δ*omcA* located at −206 mV shifted from E_p of RF for WT in the opposite direction against Sq formation (Fig. S5*C*). This effect of MtrC and OmcA protein deletion on E_p value indicates that RF interacts rather with OmcA protein compared with MtrC protein in the form of Sq. Together, the absence of a redox peak assigned to free RF for the electrodes with attached cells suggests that the EET via RF is also mediated by a Sq mechanism as well as FMN, and deletion mutant analysis also suggests that RF associates with OmcA protein instead of MtrC protein.

Discussion

In this work, we studied the mechanism by which flavins accelerate EET from heme redox centers in the OM *c*-Cyt protein MtrC to electrodes. To examine the redox state of flavins associated with MtrC, we fabricated monolayer biofilms of *S. oneidensis* strain MR-1 that were subjected to whole-cell DPV under physiological conditions. The obtained $\Delta E_{p/2}$ in the DPV signals of FMN indicates that Sq species are formed at the cell/electrode interface (Fig. 2*B*). The assignment of the E_p at −145 mV to the Ox/Sq redox reaction was confirmed by experiments using a free-radical scavenger and EPR spectroscopy (Figs. S2 and S3, respectively). The formation of Sq was not observed for the Δ*mtrC* deletion mutant (Fig. 4*A*), indicating that the Sq functions as a redox cofactor in the scaffold of MtrC. This conclusion is in harmony with the Sq stabilization in flavodoxins as a redox cofactor, which is reported for a model FMN-binding protein (24, 30). In flavodoxins the E_p of the Ox/Sq couple is generally shifted to more positive potential from that of FMN in aqueous solution as high as −50 mV (30), and it has been demonstrated by site-directed mutagenesis that the E_p shift in flavodoxins in *Desulfovibrio vulgaris* is promoted by the nonpolar environments of the protein pocket and π–π stacking interactions with aromatic amino acids (24). The Ox/Sq redox couple was also found to be a major conduit for bacterial respiratory EET at the cell/electrode interface (Fig. 5*A*). Moreover, we found that the Sq formation in MtrC protein scaffolds showed good agreement with the lactate concentration (Fig. 6). It is, therefore, most plausible that a cell-secreted flavin molecule is adsorbed specifically by the MtrC protein with reduced hemes in the presence of lactate, and the redox cycling of Ox and Sq at E_p = −145 mV (n = 1) enhances the rate and extent of EET reaction (Fig. 1*B*). However, in the absence of an electron donor (lactate), flavins are released from OM proteins following the formation of oxidized hemes in MtrC protein (Fig. S6). Experiments with RF suggested that, as with FMN, the one-electron EET mechanism holds true also for RF via an association with the OmcA protein, but not with the MtrC protein (Fig. S5).

Our present findings are consistent with reported data indicating that the addition of flavin enhances both microbial current generation via the MtrC pathway and the enzymatic reduction rate of electrodes and iron oxides by purified MtrC protein (10, 12, 15). However, based on our findings the reaction scheme and energy diagram of flavin-mediated EET (Fig. 1*B*) is not consistent with previous reports that assume that flavins mediate a two-electron redox reaction using the Ox/Hq redox couple at E_p = −260 mV (n = 2) (Fig. 1*A*).

To demonstrate the importance of one-electron reduction of electrodes in the EET process of strain MR-1, we will examine the differences in ET kinetics between EET processes mediated by the redox couples Ox/Sq and Ox/Hq based on kinetic analysis.

In flavin-mediated EET processes, it seems that MtrC protein reduces flavins to either Sq ([**1**]) or Hq ([**2**]). Breuer et al. (31) have estimated, using a large-scale molecular dynamics simulation technique, the redox potential of a heme center in MtrF protein located next to the flavin binding site as +80 mV on the basis of coordination environment of the heme in MtrF crystal structure. Considering the differences in redox potential between flavins and the heme in MtrF, flavin reduction by MtrC may be the rate-determining process in EET, because the ET from flavin to an ITO electrode (poised at +0.4 V vs. SHE) is a highly exergonic reaction. The first-order rate constants for the forward (k_f) and back reactions (k_b) for bimolecular ET are described in Eqs. **3** and **4** on the basis of the Arrhenius equation, as follows:

$$k_f = k_0 \exp\left[-\frac{\alpha n F}{RT}\Delta E\right] \quad [3]$$

$$k_b = k_0 \exp\left[\frac{(1-\alpha) n F}{RT}\Delta E\right], \quad [4]$$

where k_0 is a standard rate constant, n is the number of electrons, α is an electron transfer coefficient, and ΔE is the potential difference between the E_p values of flavin and the heme in MtrC protein. Overall current density (J) can be represented as the difference of the back and forward reaction kinetics, as described in the Butler–Volmer equation:

$$J = nF\left(k_f C_R - k_b C_O\right), \quad [5]$$

where F is the faradic constant and C_R and C_O are the concentrations of reductant and oxidant, respectively, corresponding to reduced and oxidized hemes, respectively, in MtrC. Assuming active microbial metabolism, the value for the back reaction should be negligible, because the concentration of oxidized heme would be markedly lowered by the continuous supply of respiratory electrons to the OmcA–MtrCAB complex (32). We calculated the k_f value as a function of the electron-donor potential for both reactions **1** and **2** using plausible α values (α = 0.4, 0.5, and 0.6) and the reported k_0 values for the electrode reaction of flavins, where k_0(Ox/Sq) = 0.1 and k_0(Ox/Hq) = 0.15 (33, 34) (Fig. S7*A*). It should be noted that the ratio of k_f(Ox/Sq) to k_f(Ox/Hq) gave a 10^3- to 10^5-fold faster ET rate for the reaction in [**1**] than that of [**2**] at the E_p of the heme located next to the flavin binding site in the MtrF protein (Fig. S7*A*). This result clearly demonstrates that the one-electron reaction of Ox/Sq could serve as a more efficient ET process compared with that mediated by the two-electron reaction of Ox/Hq under conditions of continuously supplied electrons. This conclusion is entirely consistent with the DPV results observed in Fig. 5, strongly suggesting that bacterial respiratory electrons are predominantly transferred to electrodes by Sq.

The findings from the kinetic estimation of EET also highlight the importance of the continuous influx of electrons generated by cellular metabolism to effectively generate Sq. More specifically, we plotted values of J as a function of the concentration ratio of oxidized to reduced hemes (C_O/C_R) for three α values (α = 0.4, 0.5, and 0.6) (Fig. S7*B*). As can be seen, the forward ET reaction from reduced heme to Ox does not overcome the back ET from Sq to oxidized heme before the C_O/C_R reaches less than 10^{-4}. This requirement for a large concentration gradient is because the increase in C_O leads to a significant decay of the flavin reduction rate by the fast kinetics of back ET reactions from Sq to oxidized hemes. Hence, the low concentration of oxidized hemes in MtrC is also a required condition to promote the formation of Sq. From these estimations, the continuous flow of electrons, which is a characteristic feature of active metabolism (32, 35), is also essential to effectively use Sq for EET processes, consistent with our finding that the EET activation by flavin is coupled with the reduction of hemes in MtrC proteins.

The heme-oxidation-state dependence on the extent of the EET process is a reasonable strategy to maintain the intracellular redox environments (redox homeostasis), because the oxidation state of hemes in MtrC reflects the balance between the electron input from respiration and the output by EET. When active metabolism accumulates electrons inside cells, the extent of EET is enhanced by the fast kinetics of Ox/Sq and continuous electron flow (Fig. S8*A*). In contrast, EET significantly slows down by the large energy barrier of Ox/Hq reaction under oxidative intercellular conditions in the absence of lactate (Fig. S8*B*). Such a regulation mechanism for the EET process would be important for microbes to accommodate or survive in diverse subsurface environments with such highly positive redox potentials (1). Our present study has not only shed light on the mechanism by which MtrC-bound flavins mediate the EET process but has also revealed the capacity of MR-1 cells to use flavin as a regulator to control the extent of EET processes in agreement with the intracellular redox environment.

Materials and Methods

Cell Preparation. *S. oneidensis* strain MR-1 was grown overnight aerobically in 10 mL of LB medium (20 g·L^{-1}) at 30 °C. The resulting cell suspension was centrifuged at 3,500 × *g* for 10 min to pellet cells, and the LB medium was then replaced with 10 mL of DM (36). The cells were further cultivated aerobically at 30 °C for 10 h using lactate (10 mM) as the sole carbon source. The suspension was centrifuged and the cells were then washed with DM before use in electrochemical experiments. Mutant strains of MR-1 lacking complete genes for MtrC and SO3177 were previously constructed by allele replacement using a two-step homologous recombination method (28, 37). The growth procedures for the two mutant strains were the same as described for the WT MR-1 strain. Metabolic inhibitor for Mtr pathway, HQNO (>99% purity; Santa Cruz Biotech), was used as aliquots from a stock solution of 50 mM in ethanol/water (50/50, vol/vol).

Electrochemical Measurements. A single-chamber, three-electrode system was used for the electrochemical studies of intact cells (16, 38). A tin-doped In_2O_3 (ITO) substrate (surface area of 3.1 cm^2) was used as a working electrode and was placed at the bottom of the reactor. Ag/AgCl (KCl saturated) and a platinum wire were used as reference and counter electrodes, respectively. Five milliliters of DM containing lactate (10 mM) was added into the electrochemical cell as an electrolyte and was deaerated by bubbling with N_2 for >30 min. The reactor temperature was maintained at 30 °C and no agitation was made during the measurements. Differential pulse voltammetry was conducted with an automatic polarization system (HZ-5000; Hokuto Denko), using 5.0-mV pulse increments, 50-mV pulse amplitude (ΔE_{pa}), 300-ms pulse width, and a 5.0-s pulse period. As a redox potential E_0 is approximated with the equation $E_0 = E_p - (\Delta E_{pa}/2)$ (21), E_0 is estimated to be 25 mV more negative than E_p observed in DP voltammograms. Measurements were made for sampling for 10 ms after each pulse. Charging current subtraction was conducted using analysis software (HZ-5000ANA; Hokuto Denko), where charging current was approximated to be a linear function.

Confocal Fluorescence Microscopy. Microscopic observations were performed on a confocal laser scanning microscope (IX-71; Olympus,) (17). Image stacks were obtained using a 60× objective. GFP fluorescence was collected with a 505- to 530-nm band-pass filter after laser excitation at 420 nm. Plane views with side profile slices were generated using Andor iQ software (version 1.9; Andor Technology).

Electron Paramagnetic Resonance Spectroscopy. X-band ESR spectra were recorded with a JEOL ES-RE2× ESR spectrometer at 77 K with a microwave power of 3.0 μW, 9.5 GHz microwave frequency, and field modulation amplitude of 0.3 mT (at 100-kHz modulation frequency). Cells were suspended in DM buffer containing 16 μM FMN, 10 mM lactate, 2 mM Fe_2O_3 powder, and 50% (vol/vol) glycerol. Samples were frozen at 77 K after 1 h of anaerobic inoculation. The spectrum of the cell suspension with 50% (vol/vol) glycerol was used as a spectral reference.

ACKNOWLEDGMENTS. We thank Prof. K. Watanabe, Dr. A. Kozuma, and Mr. G. J. Newton for the ΔSO3177 and Δ*mtrC* mutants. We also thank Prof. Y. Nosaka for the support in EPR measurements. This work was financially supported by the Exploratory Research for Advanced Technology program of the Japan Science and Technology Agency and partially by a Research Fellowship from the Japan Society for Promotion of Science for Young Scientists, Grant-in-Aid for Scientific Research 00218864.

1. Nealson KH, Saffarini D (1994) Iron and manganese in anaerobic respiration: Environmental significance, physiology, and regulation. *Annu Rev Microbiol* 48:311–343.
2. Lovley DR, Nevin KP, Woodard TL, Franks AE, Summers ZM (2010) Microbial electrosynthesis: Feeding microbes electricity to convert carbon dioxide and water to multicarbon extracellular organic compounds. *Mbio* 1(2):E00103–E00110.
3. Lovley DR (2006) Bug juice: Harvesting electricity with microorganisms. *Nat Rev Microbiol* 4(7):497–508.
4. Newton GJ, Mori S, Nakamura R, Hashimoto K, Watanabe K (2009) Analyses of current-generating mechanisms of *Shewanella loihica* PV-4 and *Shewanella oneidensis* MR-1 in microbial fuel cells. *Appl Environ Microbiol* 75(24):7674–7681.
5. Bretschger O, et al. (2007) Current production and metal oxide reduction by *Shewanella oneidensis* MR-1 wild type and mutants. *Appl Environ Microbiol* 73(21): 7003–7012.
6. Heidelberg JF, et al. (2002) Genome sequence of the dissimilatory metal ion-reducing bacterium *Shewanella oneidensis*. *Nat Biotechnol* 20(11):1118–1123.
7. Myers CR, Myers JM (1992) Localization of cytochromes to the outer membrane of anaerobically grown *Shewanella putrefaciens* MR-1. *J Bacteriol* 174(11):3429–3438.
8. Myers CR, Myers JM (1997) Outer membrane cytochromes of *Shewanella putrefaciens* MR-1: spectral analysis, and purification of the 83-kDa c-type cytochrome. *Biochim Biophys Acta* 1326(2):307–318.
9. Shi LA, et al. (2009) The roles of outer membrane cytochromes of *Shewanella* and *Geobacter* in extracellular electron transfer. *Env. Microbiol. Rep.* 1(4):220–227.
10. Coursolle D, Baron DB, Bond DR, Gralnick JA (2010) The Mtr respiratory pathway is essential for reducing flavins and electrodes in *Shewanella oneidensis*. *J Bacteriol* 192(2):467–474.
11. von Canstein H, Ogawa J, Shimizu S, Lloyd JR (2008) Secretion of flavins by *Shewanella* species and their role in extracellular electron transfer. *Appl Environ Microbiol* 74(3):615–623.
12. Marsili E, et al. (2008) *Shewanella* secretes flavins that mediate extracellular electron transfer. *Proc Natl Acad Sci USA* 105(10):3968–3973.
13. Hartshorne RS, et al. (2007) Characterization of *Shewanella oneidensis* MtrC: A cell-surface decaheme cytochrome involved in respiratory electron transport to extracellular electron acceptors. *J Biol Inorg Chem* 12(7):1083–1094.
14. Clarke TA, et al. (2011) Structure of a bacterial cell surface decaheme electron conduit. *Proc Natl Acad Sci USA* 108(23):9384–9389.
15. Ross DE, Brantley SL, Tien M (2009) Kinetic characterization of OmcA and MtrC, terminal reductases involved in respiratory electron transfer for dissimilatory iron reduction in *Shewanella oneidensis* MR-1. *Appl Environ Microbiol* 75(16):5218–5226.
16. Okamoto A, Nakamura R, Ishii K, Hashimoto K (2009) *In vivo* electrochemistry of C-type cytochrome-mediated electron-transfer with chemical marking. *ChemBioChem* 10(14):2329–2332.
17. Okamoto A, Nakamura R, Hashimoto K (2011) *In-vivo* identification of direct electron transfer from *Shewanella oneidensis* MR-1 to electrodes via outer-membrane OmcA-MtrCAB protein complexes. *Electrochim Acta* 56(16):5526–5531.
18. Bard AJ, Faulkner LR (1980) *Electrochemical Methods: Fundamentals and Applications* (Wiley, New York).
19. Li SL, et al. (2010) Effects of oxygen on *Shewanella decolorationis* NTOU1 electron transfer to carbon-felt electrodes. *Biosens Bioelectron* 25(12):2651–2656.
20. Zhao Y, et al. (2010) Three-dimensional conductive nanowire networks for maximizing anode performance in microbial fuel cells. *Chemistry* 16(17):4982–4985.
21. Rifkin SC, Evans DH (1976) Analytical evaluation of differential pulse voltammetry at stationary electrodes using computer-based instrumentation. *Anal Chem* 48(14): 2174–2180.
22. Anderson RF (1983) Energetics of the one-electron reduction steps of riboflavin, FMN and FAD to their fully reduced forms. *Biochim Biophys Acta* 722(1):158–162.
23. Ludwig ML, Andersen RD, Mayhew SG, Massey V (1969) The structure of a clostridial flavodoxin. I. Crystallographic characterization of the oxidized and semiquinone forms. *J Biol Chem* 244(21):6047–6048.
24. Zhou ZM, Swenson RP (1996) The cumulative electrostatic effect of aromatic stacking interactions and the negative electrostatic environment of the flavin mononucleotide binding site is a major determinant of the reduction potential for the flavodoxin from *Desulfovibrio vulgaris* [Hildenborough]. *Biochemistry* 35(50):15980–15988.
25. Burton GW, Joyce A, Ingold KU (1983) Is vitamin E the only lipid-soluble, chain-breaking antioxidant in human blood plasma and erythrocyte membranes? *Arch Biochem Biophys* 221(1):281–290.
26. Edmondson DE (1985) Electron-spin-resonance studies on flavoenzymes. *Biochem Soc Trans* 13(3):593–600.
27. Medina M, Vrielink A, Cammack R (1994) ESR and electron nuclear double resonance characterization of the cholesterol oxidase from Brevibacterium sterolicum in its semiquinone state. *Eur J Biochem* 222(3):941–947.
28. Kouzuma A, Meng XY, Kimura N, Hashimoto K, Watanabe K (2010) Disruption of the putative cell surface polysaccharide biosynthesis gene SO3177 in *Shewanella oneidensis* MR-1 enhances adhesion to electrodes and current generation in microbial fuel cells. *Appl Environ Microbiol* 76(13):4151–4157.
29. Marritt SJ, et al. (2012) A functional description of CymA, an electron-transfer hub supporting anaerobic respiratory flexibility in *Shewanella*. *Biochem J* 444(3):465–474.
30. Swenson RP, Krey GD (1994) Site-directed mutagenesis of tyrosine-98 in the flavodoxin from *Desulfovibrio vulgaris* (Hildenborough): Regulation of oxidation-reduction properties of the bound FMN cofactor by aromatic, solvent, and electrostatic interactions. *Biochemistry* 33(28):8505–8514.
31. Breuer M, Zarzycki P, Blumberger J, Rosso KM (2012) Thermodynamics of electron flow in the bacterial deca-heme cytochrome MtrF. *J Am Chem Soc* 134(24):9868–9871.
32. Nakamura R, Ishii K, Hashimoto K (2009) Electronic absorption spectra and redox properties of C type cytochromes in living microbes. *Angew Chem Int Ed Engl* 48(9): 1606–1608.
33. Astuti Y, et al. (2004) Proton-coupled electron transfer of flavodoxin immobilized on nanostructured tin dioxide electrodes: Thermodynamics versus kinetics control of protein redox function. *J Am Chem Soc* 126(25):8001–8009.
34. Shinohara H, Gratzel M, Vlachopoulos N, Aizawa M (1991) Interfacial electron-transfer of flavin coenzymes and riboflavin adsorbed on textured Tio2 films. *Bioelectrochem Bioenerg* 26(2):307–320.
35. Shibanuma T, Nakamura R, Hirakawa Y, Hashimoto K, Ishii K (2011) Observation of in vivo cytochrome-based electron-transport dynamics using time-resolved evanescent wave electroabsorption spectroscopy. *Angew Chem Int Ed Engl* 50(39):9137–9140.
36. Roh Y, et al. (2006) Metal reduction and iron biomineralization by a psychrotolerant Fe(III)-reducing bacterium, *Shewanella* sp. strain PV-4. *Appl Environ Microbiol* 72(5): 3236–3244.
37. Saltikov CW, Newman DK (2003) Genetic identification of a respiratory arsenate reductase. *Proc Natl Acad Sci USA* 100(19):10983–10988.
38. Nakamura R, Kai F, Okamoto A, Newton GJ, Hashimoto K (2009) Self-constructed electrically conductive bacterial networks. *Angew Chem Int Ed Engl* 48(3):508–511.